JOURNAL OF THE ROYAL SOCIETY Interface

# Computational modelling of T-cell formation kinetics: output regulated by initial proliferation-linked deferral of developmental competence

Erica Manesso, Vijay Chickarmane, Hao Yuan Kueh, Ellen V. Rothenberg and Carsten Peterson

*J. R. Soc. Interface* 2013 **10**,
doi: 10.1098/rsif.2012.0774

JOURNAL OF THE ROYAL SOCIETY Interface

rsif.royalsocietypublishing.org

Research

**Cite this article:** Manesso E, Chickarmane V, Kueh HY, Rothenberg EV, Peterson C. 2012 Computational modelling of T-cell formation kinetics: output regulated by initial proliferation-linked deferral of developmental competence. J R Soc Interface 10: 20120774. http://dx.doi.org/10.1098/rsif.2012.0774

Received: 25 September 2012
Accepted: 24 October 2012

**Subject Areas:**
systems biology

**Keywords:**
T-cell progenitors, population dynamics, Notch response thresholds, thymus, T-cell development

**Author for correspondence:**
Carsten Peterson
e-mail: carsten@thep.lu.se

Electronic supplementary material is available at http://dx.doi.org/10.1098/rsif.2012.0774 or via http://rsif.royalsocietypublishing.org.

Royal Society Publishing
Informing the science of the future

# Computational modelling of T-cell formation kinetics: output regulated by initial proliferation-linked deferral of developmental competence

Erica Manesso[1], Vijay Chickarmane[2], Hao Yuan Kueh[2], Ellen V. Rothenberg[2] and Carsten Peterson[1]

[1]Computational Biology and Biological Physics, Department of Astronomy and Theoretical Physics, Lund University, Lund, Sweden
[2]Division of Biology, California Institute of Technology, Pasadena, CA, USA

Bone-marrow-derived progenitors must continually enter the thymus of an adult mouse to sustain T-cell homeostasis, yet only a few input cells per day are sufficient to support a yield of $5 \times 10^7$ immature T-cells per day and an eventual output of $1–2 \times 10^6$ mature cells per day. While substantial progress has been made to delineate the developmental pathway of T-cell lineage commitment, still little is known about the relationship between differentiation competence and the remarkable expansion of the earliest (DN1 stage) T-cell progenitors. To address this question, we developed computational models where the probability to progress to the next stage (DN2) is related to division number. To satisfy differentiation kinetics and overall cell yield data, our models require that adult DN1 cells divide multiple times before becoming competent to progress into DN2 stage. Our findings were subsequently tested by *in vitro* experiments, where putative early and later-stage DN1 progenitors from the thymus were purified and their progression into DN2 was measured. These experiments showed that the two DN1 sub-populations divided with similar rates, but progressed to the DN2 stage with different rates, thus providing experimental evidence that DN1 cells increase their commitment probability in a cell-intrinsic manner as they undergo cell division. Proliferation-linked shifts in eligibility of DN1 cells to undergo specification thus control kinetics of T-cell generation.

## 1. Introduction

Thymocytopoiesis is the process by which T-lymphocytes are generated in the thymus from marrow-derived progenitors circulating in the blood. This complex process is controlled by a well-orchestrated differentiation transcription programme that allows relatively few marrow-derived progenitors entering the thymus every day to undergo extensive proliferation and commitment, as genes involved in T-cell functions are activated and genes responsible for differentiation to non T-cell lineages are gradually turned off [1,2]. In detail, thymus-settling progenitors enter the thymus and generate early T-cell progenitors (ETP/DN1 stage), which in turn give rise to DN2, DN3 and DN4 cells. Subsequently, DN4 cells differentiate into double positive (DP) thymocytes, which ultimately mature into single positive T-cells (for review, see [3]).

In the last years, great progress has been made in delineating the developmental pathway of T-cell lineage commitment and in identifying transcription factors that establish and maintain their fate (for review, see [1,2]). Moreover, the clinical importance of understanding how the body maintains its supply of crucial immune cells as well as the ways thymocytopoiesis may go wrong and turn into malignant lymphomas, have inspired the development of many mathematical models [4–8]. A number of models have addressed the dynamical features of the differentiation stages, for instance with studies on the way a

periodic thymic colonization by progenitor cells guarantees the homeostasis of thymocyte population [4] or on the recovery from transient depletion of dividing T-cells in mice [5]. Alternatively, other models have attempted to describe the interactions of developing thymocytes with cellular and extracellular elements of the thymus, e.g. [6], or to characterize the regulation of proliferation and differentiation [7]. In addition, Grossman *et al.* [8] have discussed how the relative probabilities of T-cell proliferation, differentiation and death are dynamically regulated to guarantee T-cell activation and homeostasis.

Although these models have provided valuable insight into dynamical properties of thymocytopoiesis, still little is known about the process of expansion of the thymus-settling progenitors especially at the early DN1 stage, where it has been shown the cells reside for around 10 days before obviously progressing into DN2 stage [3]. Notch-pathway signalling induced by cell contact with the thymic microenvironment is known to be needed for this developmental progression, but substantial numbers of cells making this response do not appear for days, suggesting an indirect pathway or a developmental limitation on responsiveness [9,10]. Indeed, Notch signals appear to trigger different gene expression responses at different DN stages, and this provides opportunities for developmental fine-tuning by signals other than Notch. Alternatively, however, immediate responses in a minority of the new immigrants could simply occur in too few cells to be detected, and differentiating progeny that emerge at each stage throughout the DN1 precursor expansion might only appear to be delayed because more abundant precursors are available after larger numbers of cell cycles. Therefore, it has not been clear how long DN1 descendants of thymic immigrants must remain in the thymus before they become competent to respond to Notch signals by differentiating into DN2 cells.

Because it is not known whether cells have uniform access to Notch signals *in vivo*, one extreme possibility is that all DN1 cells are eligible to differentiate, but only a limited number stochastically encounter the triggering signals. Further complicating the analysis, this is not a simple developmental pipeline. Within each stage of thymocyte development, the cells undergo various numbers of cycles of proliferation, so that the steady-state populations of each type may comprise different distributions of members of earlier and later generations. The generational structure of a given population depends on both the number of cell cycles that developmental stage can include and the likelihood that a cell can exit to the next developmental stage at a given cell cycle.

In this work, we have addressed the question whether DN1 cells are eligible to progress to become DN2 cells from the first days they are settled in the thymus or whether a certain number of divisions is required before their commitment. To resolve this question, *in vivo* data published by Porritt *et al.* [11] about thymic differentiation kinetics in non-irradiated mice were exploited to model the kinetics of early T-cell progenitors. These dynamical data were combined with steady-state information about DN1 cells, e.g. the approximately 10 divisions undergone at this stage [3] and the $2 \times 10^4$-fold increase in cell number between DN1 and DN3 populations expected in 14 days [3,12]. Our model recapitulated fundamental features of thymocytopoiesis and revealed that DN1 cells must divide a certain amount of times before becoming competent to progress into DN2 stage. These findings were then tested experimentally: putative early and later-stage DN1 progenitors from the thymus were purified and their progression into DN2 was measured. The experiments showed slower DN2 progression of early DN1 progenitors, despite similar cell cycle times for the two populations of DN1 cells, as predicted by the model. These results reveal a proliferation-linked increase in developmental competence in early DN1 stages gating the transition into DN2 stage, and also encourage experimental studies to elucidate the transcriptional mechanisms underlying this feature.

## 2. Results

### 2.1. A model for T-cell generation kinetics

The DN1 stage is not thought to be a true stem-cell stage, because any given cohort of donor cells is eventually chased out of the DN1 population and replaced with the progeny of new immigrants. However, there is no evidence that adult mouse DN1 cells are a conventional transit amplifying population, either, with a fixed number of possible cell divisions before further differentiation [13,14]. We therefore considered the possibility of each cell in the population as having a finite probability between 0 and 1 of either undergoing another round of cell division within the DN1 stage, admittance to the DN2 stage, or dying (the death event includes also the possibility that a DN1 cell may take another lineage). Optimizing these parameters within the framework of our model (shown in figure 1) was used to assess how these probabilities are most probably to change with residence time in the DN1 population.

Although our main goal is to gain insight into DN1 dynamics, the computational model must also include DN2, DN3 and DN4/pDP dynamics because the data published in [11] are not in absolute value, but presented as fraction of $CD4^-8^-$ donor cells (i.e. DN donor cells). In this study, purified bone-marrow progenitors were intravenously transplanted into non-irradiated CD45-congenic recipients (see the electronic supplementary material). At different days after the transplant, recipient mice were killed and the developmental stages of intrathymic progeny derived from transplanted cells were determined. As it is not known how many injected cells effectively enter the thymus, we assumed the presence of a DN1pre subset within the intravenously injected population representing the subset of precursors competent to immigrate and begin T-cell development, i.e. thymus-settling progenitors (see [1,2]). These cells were supposed to be 100 per cent of $CD4^-8^-$ donor cells within the thymus at day 0 and 0 per cent from day 7 on. A negligible probability to die was also assumed for these cells.

Each cell compartment/population is assumed to have a homogeneous behaviour. The homeostasis of each compartment generally results from the balance between formation, either from commitment of upstream progenitors or from proliferation, and loss, ascribable either to cell death or to commitment into downstream cells. The hypothetical DN1pre compartment presents an exception: at day zero $n$ cells enter the DN1pre compartment as a *bolus*; transitioning to DN1 with a constant rate $1/\tau$ ($d^{-1}$). Deterministic population models were used to model all compartments, DN1pre, DN1, DN2, DN3 and pDP, with dynamics defined in the electronic supplementary material.

Our main goal was to test the dependence of commitment of DN1 into DN2 cells on the number of divisions undergone

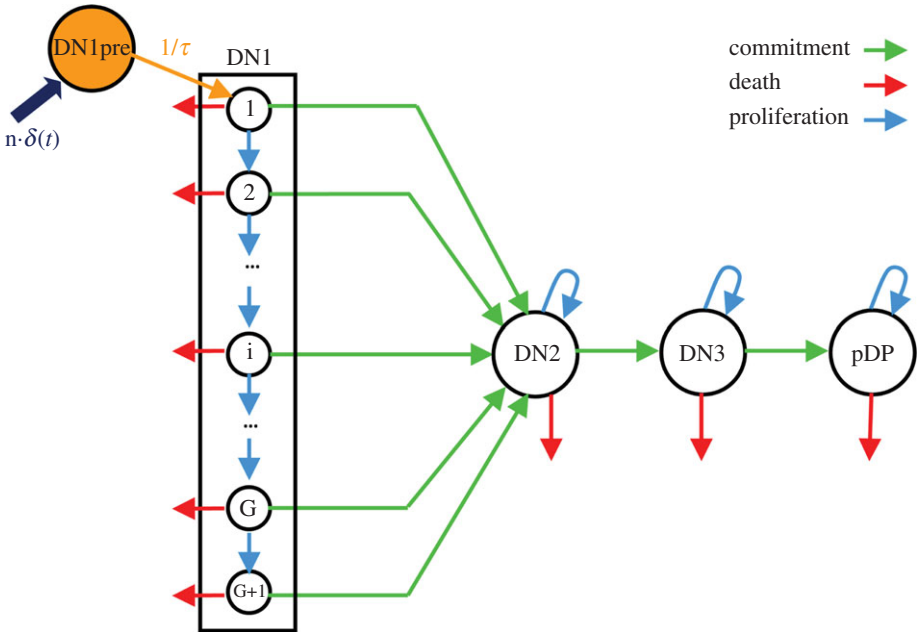


**Figure 1.** A dynamical model for T-cell progenitors in the thymus proposed to describe the data presented in [11]. At time zero, $n$ cells enter the DN1pre compartment as a *bolus* $\delta(t)$; with a constant rate $1/\tau$ ($d^{-1}$), DN1pre cells commit into DN1 cells (generation 0). DN1 cells populate $G + 1$ compartments: the generic compartment $i$, with $i = 1, \ldots, G + 1$, contains DN1 cells that have undergone $i - 1$ divisions as DN1 cells ($G$ is a parameter representing the number of generations in DN1 cell population). DN1 cells can commit to become DN2 cells, which give risen to DN3 cells. DN3 cells can commit to become pDP cells. Each DN1, DN2, DN3 or pDP cell can commit (in green), die (in red) or proliferate (in blue).

by DN1 cells within the thymic microenviroment. As a framework for this test, DN1 cells were assumed to populate $G + 1$ successive generational compartments: the generic compartment $i$, with $i = 1, \ldots, G + 1$, contains DN1 cells that have undergone $i - 1$ divisions as DN1 cells. $G$ is then a parameter representing the number of generations in DN1 cell population. Assuming that all DN1 cells have the same probability to die, we then explored two model categories for the relationship between the number of generations spent in DN1 stage and their probability to commit to become DN2 cells (see the electronic supplementary material): DN1 cells commit (A) from all generations (e.g. constantly or linearly/semi-quadratically increasing with $i$) or (B) only towards the end of the cascade (e.g. geometrically increasing with $i$ or 'only for the last generation'). The probability to proliferate was consequently calculated as one *minus* the sum of the probabilities to commit and die.

## 2.2. DN1 cells must divide a certain amount of times before becoming competent to progress into DN2 stage

Unknown parameters characterizing the models for DN1 commitment were identified by nonlinear least squares on data from [11] for different fixed number of generations $G$ (see the electronic supplementary material). According to the resulting model predictions, the models that require DN1 cells to undergo a certain number of divisions before committing into DN2 cells clearly performed better, in terms of the Akaike index AIC (which weights the number of parameters against the error related to the model prediction, electronic supplementary material, figure S1), than the models in which early-generation DN1 cells are more similar in competence to differentiate. Specifically, geometrically increasing probability of commitment ($AIC = -1.25$ for $G = 12$) and commitment 'only for the last generation' ($AIC = -1.42$ for $G = 11$) all provide a better description of the data (figure 2 shows the best model predictions versus the data) than the best fit variants of the models with commitment possible since the first generations, i.e. constant ($AIC = 1.72$ for $G = 11$), linear ($AIC = 1.75$ for $G = 12$) and semi-quadratic models ($AIC = -0.64$ for $G = 14$).

## 2.3. General features of thymocytopoiesis

The parameters estimated by the two best models that allow DN1 cells to commit only after a certain number of divisions (see below), generally matched with information available from the literature about thymocytopoiesis. Table 1 summarizes mean values for these parameters obtained by averaging solutions for different $G$ sharing a low Akaike index within the same model for the commitment of DN1 cells (see the electronic supplementary material). The very narrow standard errors of the means (s.e.m.) reflected how these models are very similar in properly describing the data besides the different number of generations $G$.

### 2.3.1. DN1pre compartment size and turnover rate

The number $n$ of cells injected in DN1pre compartment was around 200 (table 1), comparable to the number of specific intrathymic microenviromental niches [15,16]. Moreover, the 2–3 days required for DN1pre cells to become DN1 cells ($\tau$, table 1) constituted a reasonable amount of time for immigrant precursors or thymus-settling progenitors to mature in the niches [1,2].

### 2.3.2. Cell cycle times

DN2 and pDP cells cycled faster (less than 1 day) than all the other cells, consistent with evidence that DN2 and pDP cells

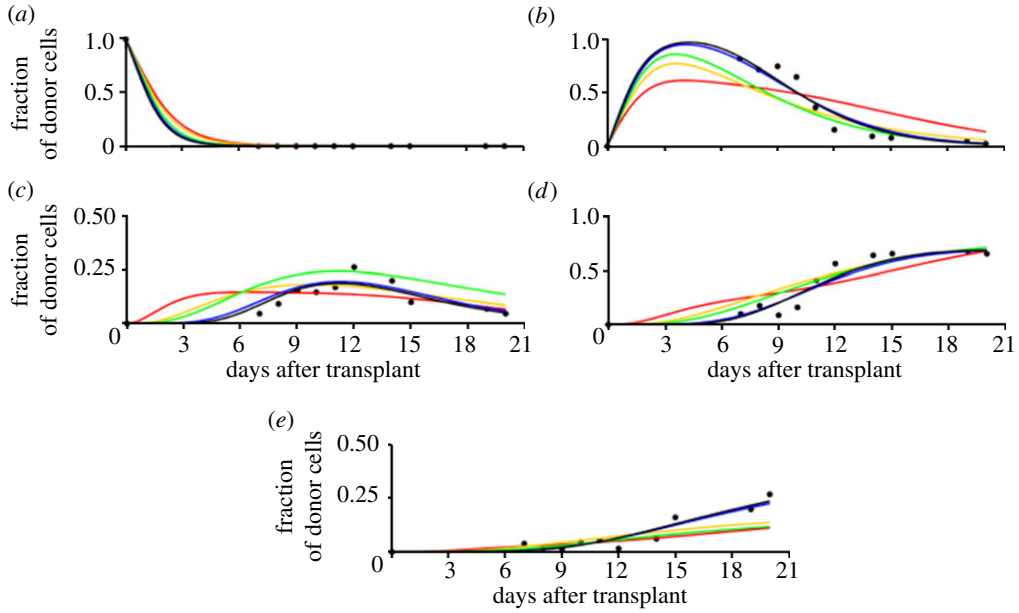


**Figure 2.** Model predictions for (*a*) DN1pre, (*b*) DN1, (*c*) DN2, (*d*) DN3 and (*e*) pDP cells in constant (red, $G = 11$), linear (yellow, $G = 12$), semi-quadratic (green, $G = 12$), geometric (blue, $G = 12$) and 'only last generation' (black, $G = 11$) best models in terms of $G$, the number of generations. Data (black dots) adapted from [11].

**Table 1.** Average parameter values (mean $\pm$ s.e.m.) in the models that allow DN1 cells to commit only after a certain number of divisions. The mean values are obtained by averaging solutions for different $G$ sharing a low Akaike index within the same model for commitment of DN1 cells.

| description | parameter | unit | geometric | only last generation |
|---|---|---|---|---|
| probability to commit for DN2 cells | $c_{DN2}$ | dimensionless | $0.60 \pm 0.02$ | $0.58 \pm 0.02$ |
| probability to commit for DN3 cells | $c_{DN3}$ | dimensionless | $0.284 \pm 0.009$ | $0.216 \pm 0.002$ |
| probability to commit for pDP cells | $c_{cDP}$ | dimensionless | $0.466 \pm 0.002$ | $0.480 \pm 0.004$ |
| probability to die for DN1 cells | $d_{DN1}$ | dimensionless | $0.13 \pm 0.02$ | $0.14 \pm 0.02$ |
| probability to die for DN2 cells | $d_{DN2}$ | dimensionless | $0.033 \pm 0.010$ | $0.028 \pm 0.007$ |
| probability to die for DN3 cells | $d_{DN3}$ | dimensionless | $0.227 \pm 0.009$ | $0.216 \pm 0.002$ |
| probability to die for pDP cells | $d_{dDP}$ | dimensionless | $0.089 \pm 0.005$ | $0.073 \pm 0.004$ |
| cycle time for DN1 cells | $T_{DN1}$ | day | $1.07 \pm 0.07$ | $1.10 \pm 0.09$ |
| cycle time for DN2 cells | $T_{DN2}$ | day | $0.685 \pm 0.018$ | $0.631 \pm 0.023$ |
| cycle time for DN3 cells | $T_{DN3}$ | day | $2.73 \pm 0.20$ | $2.65 \pm 0.07$ |
| cycle time for pDP cells | $T_{pDP}$ | day | $0.581 \pm 0.007$ | $0.514 \pm 0.014$ |
| mean transit time for DN1pre cells | $MTT_{DN1pre}$ | day | $2.50 \pm 0.13$ | $2.26 \pm 0.11$ |
| mean transit time for DN1 cells | $MTT_{DN1}$ | day | $9.76 \pm 0.04$ | $9.69 \pm 0.09$ |
| mean transit time for DN2 cells | $MTT_{DN2}$ | day | $2.47 \pm 0.06$ | $2.75 \pm 0.09$ |
| mean transit time for DN3 cells | $MTT_{DN3}$ | day | $1.68 \pm 0.09$ | $1.69 \pm 0.12$ |
| mean transit time for pDP cells | $MTT_{pDP}$ | day | $0.599 \pm 0.010$ | $0.597 \pm 0.021$ |
| number of cells entering DN1pre as a *bolus* | $n$ | cell | $194 \pm 13$ | $183 \pm 17$ |
| time of exit from DN1pre | $\tau$ | day | $2.51 \pm 0.13$ | $2.27 \pm 0.11$ |
| number of DN1pre cells in steady state | $N_{DN1pre}$ | cell | $1.25 \times 10^2 \pm 6.60 \times 10^0$ | $1.13 \times 10^2 \pm 5.69 \times 10^0$ |
| number of DN1 cells in steady state | $N_{DN1}$ | cell | $2.99 \times 10^4 \pm 1.54 \times 10^3$ | $2.73 \times 10^4 \pm 2.00 \times 10^3$ |
| number of DN2 cells in steady state | $N_{DN2}$ | cell | $2.75 \times 10^4 \pm 1.35 \times 10^3$ | $2.88 \times 10^4 \pm 3.23 \times 10^3$ |
| number of DN3 cells in steady state | $N_{DN3}$ | cell | $3.24 \times 10^6 \pm 2.94 \times 10^5$ | $2.63 \times 10^6 \pm 5.88 \times 10^5$ |
| number of pDP cells in steady state | $N_{pDP}$ | cell | $1.87 \times 10^6 \pm 3.42 \times 10^5$ | $1.57 \times 10^6 \pm 3.63 \times 10^5$ |

include a much higher cycling percentage than other DN subsets [17,18]. In comparison, DN1 cells divided every 1 day, consistent with other evidence [3], and DN3 cells were estimated to divide every 2–3 days (table 1).

### 2.3.3. Probabilities to die, commit and proliferate

Figure 3 shows the calculated probabilities to commit, proliferate and die for DN1 cells as function of the number of cell divisions (generations). DN1 cells started to commit

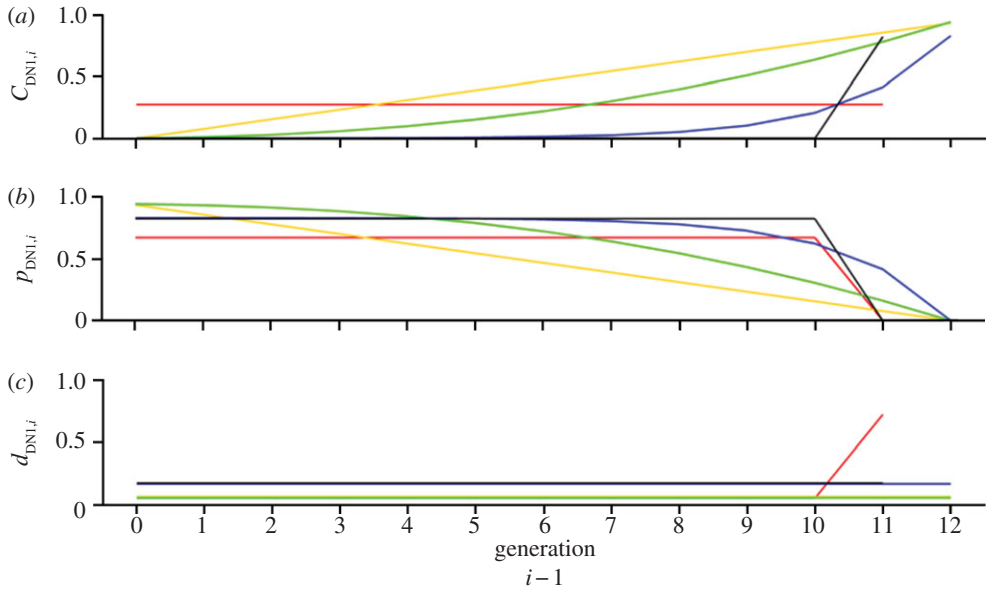


**Figure 3.** Probabilities to (*a*) die, (*b*) commit and (*c*) proliferate for DN1 cells as function of the number of generations (i.e. cell divisions) in constant (red, $G = 11$), linear (yellow, $G = 12$), semi-quadratic (green, $G = 12$), geometric (blue, $G = 12$) and 'only last generation' (black, $G = 11$) best models in terms of $G$, the number of generations.

after seven divisions in the optimal geometric model and after 10 divisions in the 'only last generation' model and the probabilities to proliferate symmetrically started to decay at the corresponding generation 7 and 10, respectively. The probability to die was around 0.13–0.14 for DN1 cells, consistent with a generally low death rate for DN1 cells. As for the other thymocytes (table 1), DN2 cell population dynamics could be fit with only a small probability to die (around 0.03); so *ca* 40 per cent DN2 cells proliferated while the remaining 60 per cent committed into DN3 cells. A higher fraction of DN3 cells died (*ca* 20%) when compared with DN2 cells, while around 50 per cent of DN3 cells proliferated and the remaining 30 per cent committed into pDP cells. The final compartment of the analysis (assumed to be pDP cells) could be fit with similar probabilities to those in the DN2 compartment, that is, a small probability to die (0.07–0.09) versus a high probability to commit (*ca* 0.5).

### 2.3.4. Mean transit times

As measured in [11], the mean transit time of DN1 cells was around 10 days, while thymocytes stayed in the DN2 stage just for a few days (table 1). Although differentiation of thymic-homing progenitors to the DP stage required around 17 days for completion according to our predictions (table 1), the mean transit times estimated for DN3 cells (2 days) and pDP cells (less than 1 day) are not completely reliable as the available time points were not enough to see the disappearance of the donor cells in these two differentiation stages (see the electronic supplementary material for details).

### 2.3.5. Number of donor cells

Because the dynamical equations of the model (see the electronic supplementary material, equations S1–S6) describe the number of thymocytes at a particular differentiation stage, it was possible to infer the time profiles for the number of donor cells (see the electronic supplementary material, figure S2). DN1pre cells exponentially decayed from around 200 cells at day 0 and disappeared by day 9 after transplant. DN1 cells started to increase at day 3 and peaked at day 11 (see electronic supplementary material, figure S3 for time profiles of DN1 sub-populations), while DN2 cells appeared at day 6 and crested at day 15 (around $7 \times 10^3$ cells). Differently, DN3 cell number showed a dramatic increase from day 9 to reach $8 \times 10^4$ cells at day 20. pDP donor cell number showed a similar behaviour, but in a reduced range: $2 \times 10^4$ cells at day 20.

### 2.3.6. Steady-state predictions

Assuming a constant input of 50 cells per day into DN1pre compartment, in steady state (see the electronic supplementary material, text S1), we predicted around 100 DN1pre cells, $3 \times 10^4$ DN1 and DN2 cells, $3 \times 10^6$ DN3 cells, and $2 \times 10^6$ pDP cells (table 1). These numbers match information available from the literature about thymocytopoiesis [19]. Electronic supplementary material, figure S4 depicts the distribution of DN1 cells in each sub-population in steady state. In the best 'only last generation' model, the number of cells in each sub-compartment was very low for the first generations and then increased up to $1.2 \times 10^4$ for generation 11. The best geometric model showed a similar behaviour, but in a smaller range (number of cells in generation 11 was $0.7 \times 10^4$) and with a decrease in cell number for the last generation [12]. This 'boomerang effect' characterizing the geometric model, but not the 'only last generation' model, is ascribable to the different profile for the probability to commit (figure 3*a*): in the first model, this probability started to be relevant at earlier generations than in the latter model, where it plays a role only for the last generation.

### 2.3.7. Parameter variability and steady-state sensitivity

Electronic supplementary material, figure S5 shows the parameter change between each solution included in the average and the best solution within the same model for the commitment of DN1 cells. Variability was always

within the same order of magnitude and never lower/higher than two/three times the *optimum* in the worst cases. The sensitivity tested on the increase in cell number between the first DN1 sub-compartment and DN3 compartment in steady state revealed that this value was more sensitive to those parameters characterizing the size of DN3 population, e.g. the probability for commit for DN2 and DN3 cells, the probability to die for DN3 cells and the number of generations (see the electronic supplementary material, figure S6). Interestingly, the cell cycle times did not affect the sensitivity parameter as they appear as ratio in electronic supplementary material, equation S20.

#### 2.3.8. Testing model assumptions

Is this the only kind of model that can satisfy the population flux parameters? The assumption that DN1 cells have constant probability to die was tested in the model where the probability to commit for DN1 cells geometrically increases with the number of divisions (in the model where the commitment is only accessible for the last generation, the probability to die increases with *i*, figure 3*c*). As the probability to proliferate was assumed constant and the sum of the three probabilities must equal to one, the probability to die decreased with the number of divisions (see the electronic supplementary material, figure S7). This gave a good fit for all but the DN1pre population (electronic supplementary material, figure S8); however, the best such model failed in respecting the $2 \times 10^4$-fold increase in cell number between DN1 and DN3 populations expected in 14 days [3,12] (estimated fold increase: 114; AIC = 1.91). We also checked the effect of a short cell-cycle time for DN1 cells (e.g. $T_{DN1}$ equals 11 h versus the estimated approx. 24 h) in the best models (see the electronic supplementary material, figures S7 and S8). In this context, all model predictions resulted in shifts towards the left side, creating a distorting acceleration in the formation of DN1 and downstream populations (AIC = 0.64 in the geometric model, 0.61 in the 'only last generation' model). Therefore, the rate of progression and extent of overall population increase are better matched by our model than by models with altered cycle times and death rates.

### 2.4. Distinct populations of DN1 progenitors show different commitment probabilities *in vitro*

Our modelling results predict that the probability of DN1 progenitors to commit to the DN2 stage does not remain constant across all generations, but instead increases with cell division. Such an increase in commitment probability may be modulated by cell-extrinsic influences, such as environmental changes that occur when progenitors migrate to a new thymic region; alternatively, it may be controlled by cell-intrinsic regulatory factors that increase the propensity for progenitors to commit as they divide. To test whether the commitment probability of DN1 progenitors increases with generation, and whether cell-intrinsic factors play a role in modulating this increase, we purified putative early and later-stage DN1 progenitors from the thymus and measured their commitment probabilities in an *in vitro* differentiation assay, where they are all subject to the same environmental conditions (see the electronic supplementary material, figure S9). For early-stage progenitors, we examined DN1 thymocytes expressing the tyrosine kinase receptor Flt3 ($Flt3^+cKit^+CD25^-$); these immature $Flt3^+$DN1 thymocytes share a similar molecular signature with candidate thymus-settling progenitors from bone marrow, and still retain some potential to differentiate into B-cells [20,21]. For later-stage progenitors, we used $Flt3^-$ DN1 thymocytes, which no longer harbour B-cell differentiation potential [9,21]. We cultured $Flt3^+$ DN1 (early), $Flt3^-$ DN1 (late) and DN2 thymocytes (positive control) on Op9-DL1 stromal cell monolayers—a feeder system that provides a uniform signalling environment to promote T-cell development [22]—and analysed their developmental kinetics at later time points using flow cytometry.

Using flow cytometry analysis, we found that starting $Flt3^-$ DN1 thymocytes showed faster progression to the DN2 stage ($CD25^+$) compared with $Flt3^+$ DN1 thymocytes over time (figure 4*a*,*b*). A significant percentage of starting $Flt3^-$ DN1 thymocytes had progressed to DN2 by day 2 (47%), and, by day 4, most of them had already progressed to DN2 (92%). By contrast, $Flt3^+$ DN1 thymocytes gave rise to lower percentages of DN2 cells on day 2 (24%) and day 4 (65%), with a significant population still remaining in DN1 on day 4 (figure 4*a*, top left). As expected, starting DN2 thymocytes either remained in DN2 or progressed to DN3 (figure 4*a*, right). Faster DN2 progression of $Flt3^-$ DN1 thymocytes compared with $Flt3^+$ DN1 thymocytes may reflect a higher probability of commitment, as predicted by the models; alternatively, it may reflect a faster cell division rate, which, given a constant probability of commitment at each cell cycle, would give rise to the increased percentage of CD25 cells (figure 4*b*). To distinguish between these two possibilities, we directly measured the cell division rates of the $Flt3^-$ and the $Flt3^+$ DN1 thymocytes using a cell proliferation dye (CellTrace Violet) that stains the starting cell population and dilutes out with each cell division. Using flow cytometry analysis, we found that $Flt3^-$ and $Flt3^+$ DN1 thymocytes diluted out the cell-bound proliferation tracking dye to similar extents after 2 or 4 days in culture (figure 4*a*, bottom), indicating that these two populations divide at similar rates. Furthermore, by estimating the mean number of cell divisions using the relative fluorescence intensities of the dye in the starting and final cell populations, we also found that $Flt3^-$ and $Flt3^+$ DN1 thymocytes divided a similar number of times over the first four days in culture (figure 4*c*). These data indicate that DN1 progenitors indeed increase their commitment probability as they progress from an earlier ($Flt3^+$) to later stage ($Flt3^-$), consistent with model predictions, and further indicate that this increase in commitment probability is controlled, at least in part, by cell-intrinsic regulatory factors.

## 3. Discussion

Every day around 50 marrow-derived progenitors enter the thymus of an adult mouse to sustain T-cell homeostasis in organs and tissues. Recently, significant progress has been made to delineate the developmental pathway of T-cell lineage commitment (for review, see [1,2]), but the remarkable expansion of early T-cell progenitors in the thymus still remains obscure. In this work, we have implemented and investigated a series of computational models about T-cell differentiation stages focusing on population dynamics of early T-cell progenitors (DN1) in order to understand whether they mature into the next stage (DN2) only after a

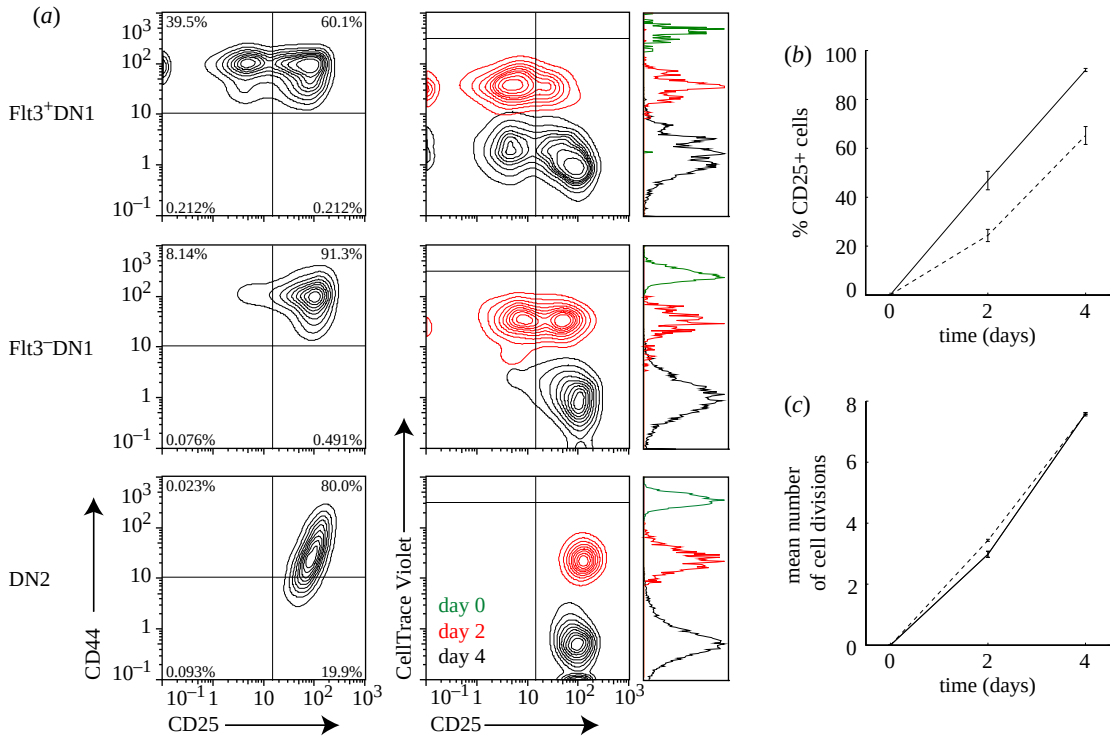


**Figure 4.** Flt3$^+$ DN1 thymocytes show a decreased probability of DN2 commitment per generation compared with Flt3$^-$ DN1 thymocytes. (*a*) Flow cytometry plots showing DN stage progression (CD44 versus CD25, top) and cell cycle progression (CellTrace Violet versus CD25, bottom) of Flt3$^+$ DN1 (left), Flt3$^-$ DN1 (centre) or DN2 (right) thymocytes cultured on Op9-DL1 stromal cell layers for the indicated number of days. (*b*) Percentage of committed (CD25$^+$) cells over time in Op9-DL1 culture of Flt3$^+$ (dashed) or Flt3$^-$ (solid line) DN1 thymocytes. (*c*) Each time point represents mean and standard deviation of two to three experiments. Plot shows a decreased percentage of committed (CD25$^+$) cells generated from Flt3$^+$ DN1 thymocytes compared with Flt3$^-$ DN1 thymocytes. Mean number of cell divisions over time in Op9-DL1 culture of Flt3$^+$ (dashed) and Flt3$^-$ (dotted) DN1 thymocytes. The mean number of cell divisions was given by the logarithm of the ratio of the initial to final mean fluorescence intensities of the CellTrace Violet-stained cell populations. Plot shows that Flt3$^+$ and Flt3$^-$ DN1 cells divide at similar rates in Op9-DL1 culture so that DN2 commitment rates per generation are intrinsically different.

certain number of divisions or beginning at the first moment they settle in the thymus. For this purpose, early T-cell progenitors were divided into different generations depending on the number of divisions undergone at the DN1 stage. Two major type of scenarios (A and B) for competence to undergo commitment were then explored: (A1) commitment at a constant rate independent of the generation, (A2) increasing linearly with generation, (A3) increasing non-linearly with generation, (B1) geometrically increasing with the number of divisions and (B2) commitment only accessible for the last generation. The latter (B1–B2) all have in common late commitment into DN2. Unknown parameters characterizing the five models were identified by best fit using data in [11]. The models that require DN1 cells to undergo a certain number of divisions before committing into DN2 cells, i.e. B1–B2, provided a better description of the data when compared with the models that allow DN1 cells to commit since the first generations, that is A1–A3 (figure 5). The effects of a decreasing probability to die and a short cell cycle time for DN1 cells were then tested: these conditions led to unreliable model predictions (e.g. inadequate fold increase between DN1 and DN3 populations and acceleration in the formation of DN1 and downstream populations, respectively) thus ensuring the robustness of our findings. The progression of DN1 cells into DN2 stage was also explored with more intricate models, such as Weibull (right skewed bell shape) and exponential distributions for the probability to commit of DN1 cells (electronic supplementary material, figures S7 and S8; AIC $= -1.10$ in the Weibull model, $-1.25$ in the exponential model). These models provided results similar to those described in this study (e.g. the Malthusian parameter in the exponential model was estimated as around 0.7, providing similar performance to the geometric model), but both share the feature of sharply increasing propensity to advance to DN2 stage at later cell cycles, thus confirming the relevance of proliferation with differentiation initially suppressed at early stages of T-cell lineage.

All satisfactory models suggested that the probability of DN1 progenitors to commit to the DN2 stage does not remain constant across all generations, but instead increases with each generation, and so this was tested experimentally: putative early and later-stage DN1 progenitors from the thymus were purified and their progression into DN2 was measured *in vitro*. For putative early-stage progenitors, we examined DN1 thymocytes expressing the tyrosine kinase receptor Flt3: these immature Flt3$^+$ DN1 thymocytes share a similar molecular signature with candidate thymus-settling progenitors from bone marrow, and still retain some potential to differentiate into B cells [20,21]. For putative later-stage progenitors, we used Flt3$^-$ DN1 thymocytes, which no longer harbour B-cell differentiation potential [9,21]. The experiments showed slower DN2 progression of early DN1 progenitors, despite similar cell cycle time for the two populations of DN1 cells. Our experimental data are consistent with our prediction that DN1 progenitors increase their commitment probability as they progress from an earlier (Flt3$^+$) to later stage (Flt3$^-$), and further argue against the

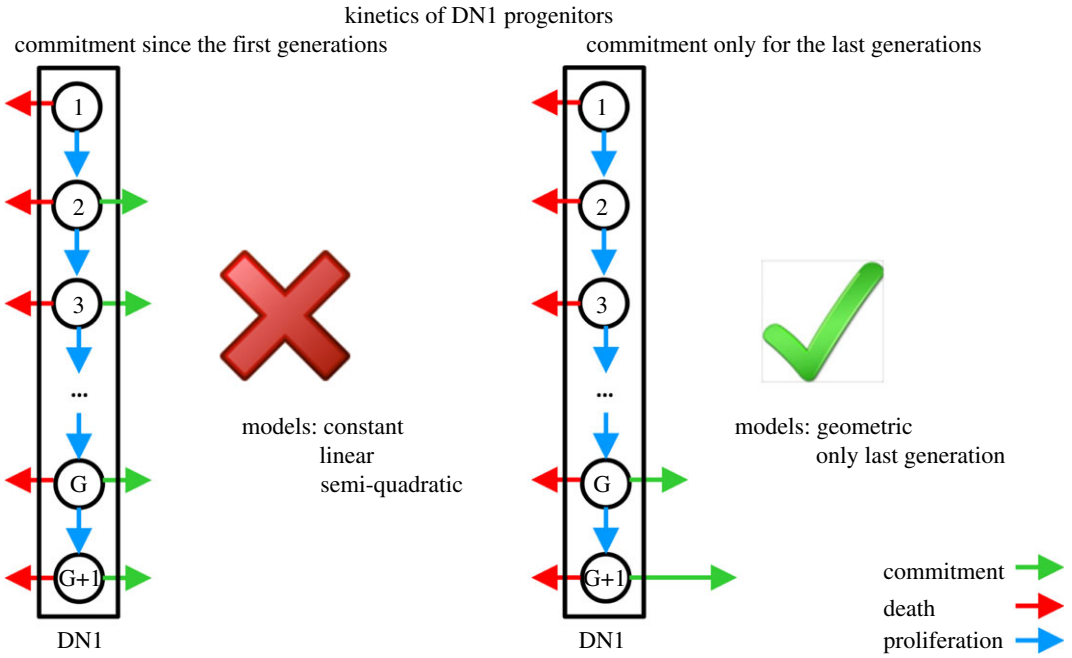


**Figure 5.** Two major type of scenarios for DN1 competence to undergo commitment were explored: commitment since the first generations (commitment at a constant rate independent of the generation, linearly with generation or semi-quadratically with generation) and commitment only for the last generations (geometrically increasing with the number of divisions or commitment only for the last generation). The latter provided a better description of thymocytopoiesis when compared with the models that allow DN1 cells to commit since the first generations. Green, commit; red, die; blue, proliferate.

'only last generation' model in favour of the geometric model for the *in vitro* system, because both $Flt3^+$ and $Flt3^-$ give rise to DN2 cells. DN1 cells can thus be read as an intermediate population between true stem cells and transit amplifying cells with increasing probability to commit.

Our model framework is based upon a number of constraints and assumptions, such as the presence of DN1pre compartment representing the immigrant precursors or thymus-settling progenitors (see [1,2]). These cells are supposed to be injected as a *bolus* at time zero and to mature into DN1 cells within a couple of days. Moreover, a constant probability to die was assumed for all DN1 cells (independently from the number of divisions), a homogeneous behaviour for cells at DN2, DN3 and pDP stages was considered, and the fold increase between DN1 and DN3 stages in 13 days following the transplant was hypothesized. With these few assumptions, we were able to reproduce fundamental features of thymocytopoiesis, such as the number of specific intrathymic microenviromental niches (corresponding to the number of injected DN1pre cells) [15] as well as the cell cycles, mean residence times and cell numbers in steady state for DN populations [11,19].

*In vivo*, several different factors could explain the steep increase in competence to differentiate from earlier to later generations of DN1 cells. Importantly, our models show that the DN1 cells are not developmentally equivalent *in vivo*. While crossing the threshold to acquire commitment capability may depend on some restricted environmental signal, its effect should be to change the cells intrinsically. Our experimental results show that the early-stage DN1 cells do intrinsically differ from later-generation DN1 cells, through their slower ability to differentiate even under uniform *in vitro* stimulation conditions. This is in agreement with evidence showing that a subset of early DN1 cells, about 10 per cent of the steady-state population, still expresses the progenitor-specific growth factor receptor Flt3 (Flk2) and maintains a capability to develop into B-cells, which is lost by later generations of DN1 cells [9,21,23,24]. While a strictly generation-counting mechanism, such as in some developmental and non-developmental systems [25–28], would need to be based on a mechanism undiscovered as yet, the geometric model could reflect the need to dilute out a differentiation inhibitor or set of inhibitors with each cell cycle. These models therefore could be tested for a definite molecular basis, and candidate inhibitors of developmental progression may be obtained by using gene-expression profiling to identify regulatory factors that are differentially downregulated at the DN2 stage [1,29].

In conclusion, our models recapitulate fundamental features of thymocytopoiesis and reveal that adult mouse DN1 cells must divide a certain amount of times before becoming competent to progress into DN2 stage. Importantly, this condition must be a point of regulation in ontogeny, for foetal T-cell precursors can generate the first DN2 progeny within about 1–2 days of entering the thymus, albeit with much less proliferative expansion [12]. By demonstrating the requirement for a mechanism delaying full onset of competence in adult T-cell precursors, our models validate the search for its molecular basis and confirm a new aspect of the role of proliferation at early stages of T-cell lineage development.

This work was supported by the Swedish Research Council (Vr 621-2008-3074), the Swedish Foundation for Strategic Research (A3 04 159p), the United States Public Health Service (NIH grant no. AI095943 (EVR)). E.M. was also supported by the Landshovding Per Westling Foundation, H.Y.K. by an Irvington Institute Fellowship of the Cancer Research Institute, and E.V.R. by the Albert Billings Ruddock Professorship of Biology. V.C. would like to acknowledge Prof. Elliot Meyerowitz for support. We thank Mary Yui and Ni Feng at Caltech for advice and assistance with thymocyte experiments. We also thank Diana Perez from the Caltech Cell Sorting Facility for cell sorting, and Rob Butler and Scott Washburn for mouse care as well as colleagues in Computational Biology at Lund University for useful discussions.

# References


1. Rothenberg EV, Moore JE, Yui MA. 2008 Launching the T-cell-lineage developmental programme. *Nat. Rev. Immunol.* **8**, 9–21. (doi:10.1038/nri2232)
2. Love PE, Bhandoola A. 2011 Signal integration and crosstalk during thymocyte migration and emigration. *Nat. Rev. Immunol.* **11**, 469–477. (doi:10.1038/nri2989)
3. Petrie HT, Zúñiga-Pflücker JC. 2007 Zoned out: functional mapping of stromal ING microenvironments in the thymus. *Annu. Rev. Immunol.* **25**, 649–679. (doi:10.1146/annurev.immunol.23.021704.115715)
4. Cai AQ, Landman KA, Hughes BD, Witt CM. 2007 T cell development in the thymus: from periodic seeding to constant output. *J. Theor. Biol.* **249**, 384–394. (doi:10.1016/j.jtbi.2007.07.028)
5. Thomas-Vaslin V, Altes HK, de Boer RJ, Klatzmann D. 2008 Comprehensive assessment and mathematical modeling of T cell population dynamics and homeostasis. *J. Immunol.* **180**, 2240–2250.
6. Souza e Silva H, Savino W, Feijoo RA, Vasconcelos ATR. 2009 A cellular automata-based mathematical model for thymocyte development. *PLoS ONE* **43**, e823. (doi:10.1371/journal.pone.0008233)
7. Bocharov G *et al*. 2011 Feedback regulation of proliferation vs. differentiation rates explains the dependence of CD4 Tcell expansion on precursor number. *Proc. Natl Acad. Sci. USA* **108**, 3318–3323. (doi:10.1073/pnas.1019706108)
8. Grossman Z, Min B, Meier-Schellersheim M, Paul WE. 2004 Concomitant regulation of T-cell activation and homeostasis. *Nat. Rev. Immunol.* **4**, 387–395. (doi:10.1038/nri1355)
9. Sambandam A, Maillard I, Zediak VP, Xu L, Gerstein RM, Aster JC, Pear WS, Bhandoola A. 2005 Notch signaling controls the generation and differentiation of early T lineage progenitors. *Nat. Immunol.* **6**, 663–670. (doi:10.1038/ni1216)
10. Thompson PK, Zúñiga-Pflücker JC. 2011 On becoming a T cell, a convergence of factors kick it up a Notch along the way. *Semin. Immunol.* **23**, 350–359. (doi:10.1016/j.smim.2011.08.007)
11. Porritt HE, Gordon K, Petrie HT. 2003 Kinetics of steady-state differentiation and mapping of intrathymic-signaling environments by stem cell transplantation in nonirradiated mice. *J. Exp. Med.* **198**, 957–962. (doi:10.1084/jem.20030837)
12. Lu M *et al*. 2005 The earliest thymic progenitors in adults are restricted to T, NK, and dendritic cell lineage and have a potential to form more diverse TCRbeta chains than fetal progenitors. *J. Immunol.* 175, 5848–5856.
13. Martins VC *et al*. 2012 Thymus-autonomous T cell development in the absence of progenitor import. *J. Exp. Med.* **209**, 1409–1417. (doi:10.1084/jem.20120846)
14. Peaudecerf L *et al*. 2012 Thymocytes may persist and differentiate without any input from bone marrow progenitors. *J. Exp. Med.* **209**, 1401–1408. (doi:10.1084/jem.20120845)
15. Foss D, Donskoy E, Goldschneider I. 2002 Functional demonstration of intrathymic binding sites and microvascular gates for prothymocytes in irradiated mice. *Int. Immunol.* **13**, 331–338. (doi:10.1093/intimm/14.3.331)
16. Goldschneider I, Komschlies KL, Greiner DL. 1986 Studies of thymocytopoiesis in rats and mice. I. Kinetics of appearance of thymocytes using a direct intrathymic adoptive transfer assay for thymocyte precursors. *J. Exp. Med.* **163**, 1–17. (doi:10.1084/jem.163.1.1)
17. O'Reilly LA, Harris AW. 1997 bcl-2 transgene expression promotes survival and reduces proliferation of CD3-CD4-CD8- T cell progenitors. *Int. Immunol.* **9**, 1291–1301. (doi:10.1093/intimm/9.9.1291)
18. Vasseur F, Campion AL, Pénit C. 2011 Scheduled kinetics of cell proliferation and phenotypic changes during immature thymocyte generation. *Eur J. Immunol.* **31**, 3038–3047. (doi:10.1002/1521-4141(2001010)31:10<3038::AID-IMMU3038>3.0.CO;2-3)
19. Lai JCY, Wlodarska M, Liu DJ, Abraham N, Johnson P. 2010 CD45 regulates migration, proliferation, and progression of double negative 1 thymocytes. *J. Immunol.* **185**, 2059–2070. (doi:10.4049/jimmunol.0902693)
20. Luc S *et al*. 2012 The earliest thymic T cell progenitors sustain B cell and myeloid lineage potential. *Nat. Immunol.* **13**, 412–419. (doi:10.1038/ni.2255)
21. Tan JB, Visan I, Yuan JS, Guidos CJ. 2005 Requirement for Notch1 signals at sequential early stages of intrathymic T cell development. *Nat. Immunol.* **6**, 671–679. (doi:10.1038/ni1217)
22. Schmitt TM, Zúñiga-Pflücker JC. 2006 T-cell development, doing it in a dish. *Immunol. Rev.* **209**, 95–102. (doi:10.1111/j.0105-2896.2006.00353.x)
23. Heinzel K, Benz C, Martins VC, Haidl ID, Bleul CC. 2007 Bone marrow-derived hemopoietic precursors commit to the T cell lineage only after arrival in the thymic microenvironment. *J. Immunol.* **178**, 858–868.
24. Ceredig R, Bosco N, Rolink AG. 2007 The B lineage potential of thymus settling progenitors is critically dependent on mouse age. *Eur J. Immunol.* **37**, 830–837. (doi:10.1002/eji.200636728)
25. Newport J, Kirschner M. 1982 A major developmental transition in early *Xenopus* embryos: I. characterization and timing of cellular changes at the midblastula stage. *Cell* **30**, 675–686. (doi:10.1016/0092-8674(82)90272-0)
26. Temple S, Raff MC. 1986 Clonal analysis of oligodendrocyte development in culture: evidence for a developmental clock that counts cell divisions. *Cell* **44**, 773–779. (doi:10.1016/0092-8674(86)90843-3)
27. Raff M. 2007 Intracellular developmental timers. *Cold Spring Harb. Symp. Quant. Biol.* **72**, 431–435. (doi:10.1101/sqb.2007.72.007)
28. Wells J, Lee B, Cai AQ, Karapetyan A, Lee W-J, Rugg E, Sinha S, Nie Q, Dai X. 2009 Ovol2 suppresses cell cycling and terminal differentiation of keratinocytes by directly repressing c-Myc and Notch1. *J. Biol. Chem.* **2845**, 29 125–29 135. (doi:10.1074/jbc.M109.008847)
29. Zhang JA, Mortazavi A, Williams BA, Wold BJ, Rothenberg EV. 2012 Dynamic transformations of genome-wide epigenetic marking and transcriptional control establish T cell identity. *Cell* **149**, 467–482. (doi:10.1016/j.cell.2012.01.056)